ISSN 0010-5082, Combustion, Explosion, and Shock Waves, 2020, Vol. 56, No. 2, pp. 220–230. © Pleiades Publishing, Ltd., 2020.
Original Russian Text © .

Shock-Wave Initiation of a Thermite Mixture of Al + CuO

S. Yu. Ananev[a], L. I. Grishin[a,b], A. Yu. Dolgoborodov[a,b,c], and B. D. Yankovskii[a]

UDC 662.215.4+534.222.2

Published in *Fizika Goreniya i Vzryva*, Vol. 56, No. 2, pp. 107–117, March–April, 2020.
Original article submitted December 18, 2018; revision submitted February 4, 2019; accepted for publication February 20, 2019.

Abstract: The shock-wave initiation of chemical reaction in pressed pellets of a stoichiometric mixture of Al and CuO powders in a steel tube was studied. The dynamics of the chemical transformations in the heterogeneous flow of reaction products of the mixture with dispersion of the pressed pellet material in the unloading wave was investigated. From the results of pyrometric measurements, the maximum brightness temperature of chemical reaction products was ≈3500 K.

Keywords: thermite compositions, shock-wave initiation, chemical reaction, detonation.

DOI: 10.1134/S0010508220020136

INTRODUCTION

Additives to individual explosives are known to influence detonation parameters and the composition of explosion products [1–3]. The nature of this influence depends largely on the time of involvement of these additives in chemical interactions with detonation products [4, 5]. A number of applications of explosives require a longer time of energy release than that when using individual explosives or their traditional mixtures [6, 7]. Additional energy release can be obtained, e.g., by using additives of aluminum or its mixtures with oxidizers ($KClO_4$, $KMnO_4$, polytetrafluoroethylene, etc.) burning up in the air behind the shock-wave front [8–11]. In recent years, the possibility of using various explosive compositions based on mechanically activated thermite mixtures of oxidizer and fuel with components mixed at the submicron level has also been studied [12].

Upon detonation of a mixture of an explosive with a thermite composition, the components of the latter are affected by both the detonation wave pressure and the high temperature of detonation products. These two factors provide an initiating impulse for chemical interaction between the components of the thermite composition. Due to the limited extent of the region of high (detonation) parameters of detonation products of explosives (pressure, temperature) [13, 14], it is sufficient to estimate the duration of their intense initiating impulse by the interval 1–2 μs.

In this work, the results obtained previously [15] were used to study the effect of shock-wave loading on chemical transformations in mixtures of Al and CuO powders.

RESEARCH MATERIAL AND LOADING MODEL

The initial components of the thermite composition were PP-2 aluminum powder (flat particles with a linear size of 50–100 μm; 2–5 μm thick) and a copper oxide (CuO) powder (analytic grade) (20–50 μm). The Al/CuO mass ratio for the preparation of the mixture corresponded to a stoichiometric proportion of 18.5/81.5. Mixing and mechanical activation of the components were carried out in a vibratory ball mill. Details of the mechanical activation of thermite mixtures are described in [15]. To prevent reaction during the treatment, hexane was added to the mix-

[a] Joint Institute for High Temperatures, Russian Academy of Sciences, Moscow, 125412 Russia; aldol@ihed.ras.ru.
[b] National Research Nuclear University MEPhI, Moscow, 115409 Russia.
[c] Semenov Federal Research Center of Chemical Physics, Russian Academy of Sciences, Moscow, 119991 Russia.

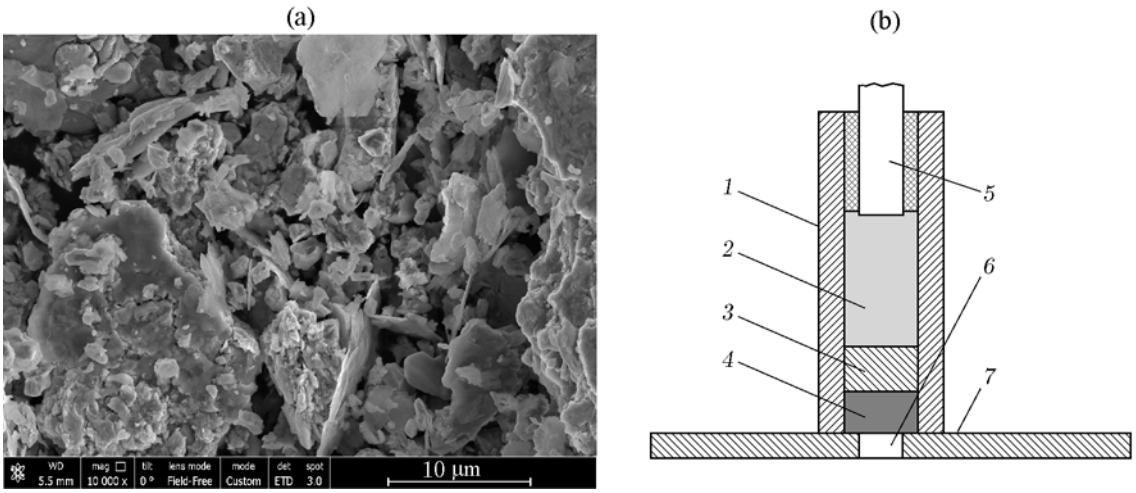

Fig. 1. Photograph of the mixture after mechanical activation (a) and a diagram of the experimental assembly for shock initiation of a pressed thermite pellet (b): (*1*) steel tube; (*2*) explosive charge; (*3*) steel piston; (*4*) thermite pellet; (*5*) detonating cord; (*6*) nozzle orifice; (*7*) steel plate.

ture and activation was carried out in cycles of 60 s. The activation time was varied from 2 to 20 min. After preparation, the mixture was dried. In some experiments, mixtures of V-Alex (100–200 nm) and nCuO (50–80 nm) nanosized components ("Peredovye Poroshkovye Tekhnologii" Ltd, Tomsk) were used.

The obtained powders consisted of a polydisperse mixture of large conglomerates of flat fragments of Al particles (≈10 μm) with CuO particles crushed to submicron sizes (Fig. 1a). Due to different strength characteristics of the materials and the scatter in particle size and shape, the conglomerates had the form of disordered structures with numerous points of contact of the components. Presumably, these points can serve as primary initiation sites of chemical interaction.

The dry mixture in an amount of 1 g was pressed into pellets with a porosity of 10–36%.

Shock-wave loading of the pressed pellet was carried out by the products of explosion of the explosive charge in a steel tube with inner and outer diameters of 8 and 14 mm (Fig. 1b). The explosive charge consisted of phlegmatized RDX with a density of ≈1.15 g/cm^3. A cylindrical steel disk between the explosive charge and the pellet served as a piston and thermal protection against hot detonation products. The steel tube was mounted on a steel plate 2.5 mm thick coaxially with the nozzle orifice in the plate. The area of the nozzle orifice S_n was varied in the range 0–1 of the area of the thermite pellet S_0. The mass ratio of the explosive charge, piston, and pellet was kept constant: 1/1/1. The mass of each element was 1 g.

The loading intensity was changed by varying the air gap (0–3 lengths of the explosive charge) between the charge and adjacent assembly elements. The unloading intensity of pellets and the degree of their subsequent dispersion in the unloading wave were varied by changing the area of the nozzle orifice. At an area of the nozzle orifice $S_n \leqslant 0.5S_0$, the steel piston stuck in the nozzle and prevented the detonation products from escaping (see position *7* in Fig. 2b).

LOADING PARAMETERS AND ENERGY DISSIPATION

Upon detonation of the explosive charge, the thermite pellet is loaded through the steel piston by a shock wave. According to [16], the Hugoniot of the initial pellet of a mixture of Al + CuO with a density of 4.24 g/cm^3 (porosity 16%) can be represented by the expression $D = 1.32 + 1.98u$ (curve *3* in Fig. 2). The initial loading pressure of the pellet is determined by the intersection point of this Hugoniot with the unloading curve of the steel piston *4* (see pressure $p_2 \approx 12$ GPa in Fig. 2). The deformation and relative movement of particles of the initial components in thermite pellets leads to partial conversion (dissipation) of shock-wave energy into heat [17, 18].

The work of deformation of the least strong component of the pellet can be estimated by the relation $A_{\text{def}} \approx \sigma_i V_i \varepsilon$, where σ_i is the yield point of the component, V_i is the volume of the component, and ε is the porosity. For Al particles ($\sigma_{\text{Al}} = 120$ MPa) at a pellet porosity of 20%, this value is ≈1.6 J.

The shock-wave energy dissipation in the Al + CuO thermite pellet was experimentally estimated by com-

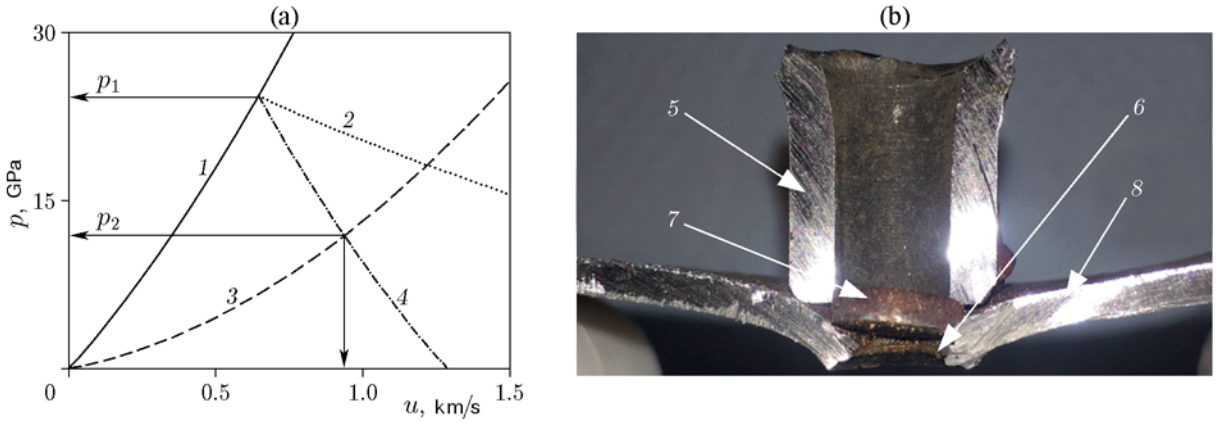

Fig. 2. (a) p–u diagram of loading of a pellet by a steel piston: (*1*) Hugoniot of the steel piston; (*2*) unloading curve of detonation products; (*3*) Hugoniot of the pellet; (*4*) unloading curve of the steel piston; p_1 is the initial shock-wave pressure in the steel piston and p_2 is the initial shock-wave pressure in the pellet; (b) elements of the assembly after shock-wave loading: (*5*) steel tube; (*6*) nozzle orifice; (*7*) steel piston; (*8*) steel plate.

paring the residual deformations of the piston and steel plate under static and shock-wave loading of the experimental assembly [19]. The steel plate in these experiments had no nozzle. Static loading of the assembly elements was carried out on an MS-1000 test press. In the experiments, the dependences of the residual stain on the applied force for each of the elements were determined. The area under these dependences determines the energy consumptions A_p and A_{def} in the deformation of the steel piston and steel plate, respectively. The calibration curves for determining the energy consumption from known strain are shown in Fig. 3 (curves *1* and *3*).

During the shock-wave loading of experimental assemblies, the initial velocity of the deformed surface of a steel plate obtained from the data of piezoelectric sensors was ≈140–150 m/s. The strain rate of the steel plate can be estimated as $5 \cdot 10^3$ s^{-1}. Residual deformation of the steel plate occurs under the action of the primary shock-wave energy that reached the plate. Due to the absence of fracture of the steel plate (Fig. 4), the energy balance can be considered under the assumption of absolutely inelastic impact:

$$E_{\text{load}} = A_p + E_{\text{fr}} + A_{\text{def}},$$

where E_{load} is the loading energy and E_{fr} is the dissipation energy in the thermite pellet. In experimental assemblies with elements of different materials, different residual strains of the steel plate occur. Comparison of these strains makes it possible to evaluate the energy dissipation in the thermite pellet. For this, the following combinations of elements were used in the experiments (see Fig. 4): a steel piston (1 g) + a steel piston (1 g); a steel piston (1 g) + an (Al + CuO) thermite pellet (1 g).

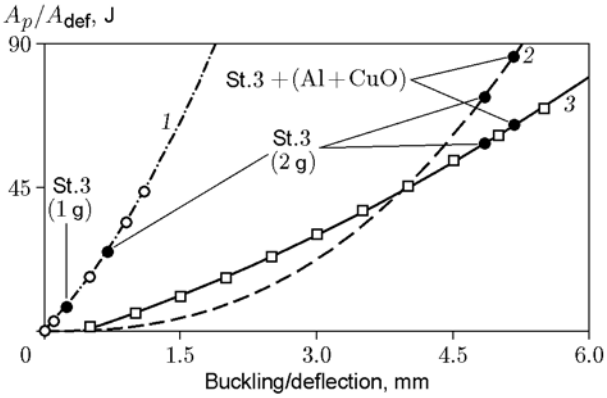

Fig. 3. Calibration dependences of the energy consumption A_p in the buckling of a steel piston with a diameter of 8 mm and a height of 5 mm (*1*) and the energy consumption A_{def} in the deflection of a steel plate 2.5 mm thick (*3*): curve *2* is plotted by relation (1) for the steel plate; the points are the results of dynamic loading experiments with different combinations of elements (see Fig. 4) in the assembly.

Assuming the same energy effect of the explosive charge on the set of elements for each of the experimental assemblies (E_{load} = const), we derived a system of two linear equations with two unknowns. The solution of the system based on experimental data and calibration dependences (see Fig. 3) determines the dissipation

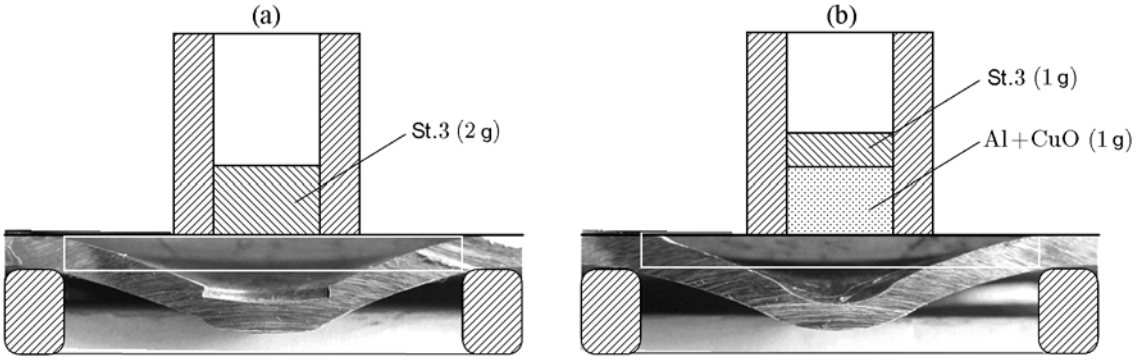

Fig. 4. Diagrams of experimental assemblies for determining the energy dissipation in a thermite pellet from residual strains of the steel piston and steel plate.

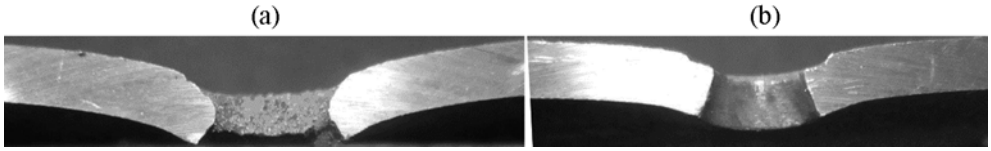

Fig. 5. Photographs of the residual strain of the nozzle part ($S_n = 0.5S_0$) of the steel plate: (a) strain after loading of an assembly consisting of a piston (weighing 1 g and thickness 2.5 mm) and a Al + CuO pellet (weighing 1 g and height 5 mm) with initiation of the reaction; (b) strain after loading of a Al + CuO pellet (weighing 2 g and height 10.5 mm) without reaction initiation.

energy $E_{\text{fr}} = 17 \pm 5$ J in a thermite pellet 5 mm thick and weighing 1 g. This value can be increased by a factor of 1.5 (dynamic coefficient) to $E_{\text{fr}} = 26 \pm 7$ J by taking into account the increase in the strength characteristics of steel elements under dynamic deformation compared with static deformation. The work of dynamic plastic deformation of the steel plate for the assemblies shown schematically in Fig. 4 can also be determined by the semi-empirical relation [20]

$$A_{\text{def}} = 471\pi R_0^2 H_0 (1.33(h/R_0)^2)^{1.23}, \qquad (1)$$

where 471 (MPa) is the empirical coefficient for St.3 steel, R_0 is the radius of the support ring, and H_0 and h are the initial thickness and depth of deflection of the steel plate.

In the case of loading of a higher thermite pellet weighing 2 g, the shock-wave energy decreases noticeably with free path, resulting in a decrease in the probability of reaction initiation in the underlying layers of the composition up to its complete decay. The absence of reaction affects the nature of the residual deformation of the nozzle part of the steel plate (Fig. 5). In this case, there is no thermal effect on the nozzle and there is a decrease in the volume of its residual plastic deformation [21].

FORMATION AND STRUCTURE OF THE FLOW

When the shock wave reaches the pellet–air interface, an unloading wave is reflected into the material of the pellet, and the pellet body is dispersed into clusters in this wave. The clusters contain different numbers of particles of components with primary initiation sites of chemical interaction. Due to the arbitrary mass distribution of clusters, they have different velocities at the edge of the experimental assembly, resulting in the formation of an extended flow of accelerated particles. This is confirmed by photographs of the expansion of the inert pellet material against the bright screen after shock-wave loading (Fig. 6a) [22]. The photographs were taken with a CORDIN-222-16 electron-optical camera. The camera produces 16 frames in a time period of up to 5 ms with an exposure of 5 ns. The snapshot in Fig. 6 was taken at a time of 1700 μs with an exposure of 1 μs. The top flow (velocity 438 m/s) was formed by accelerating a pellet weighing 1 g through a steel piston weighing 1 g. The bottom flow (velocity 437 m/s) was formed by accelerating a pellet weighing 2 g without a steel piston. The velocities of the flow front were determined by approximating the data

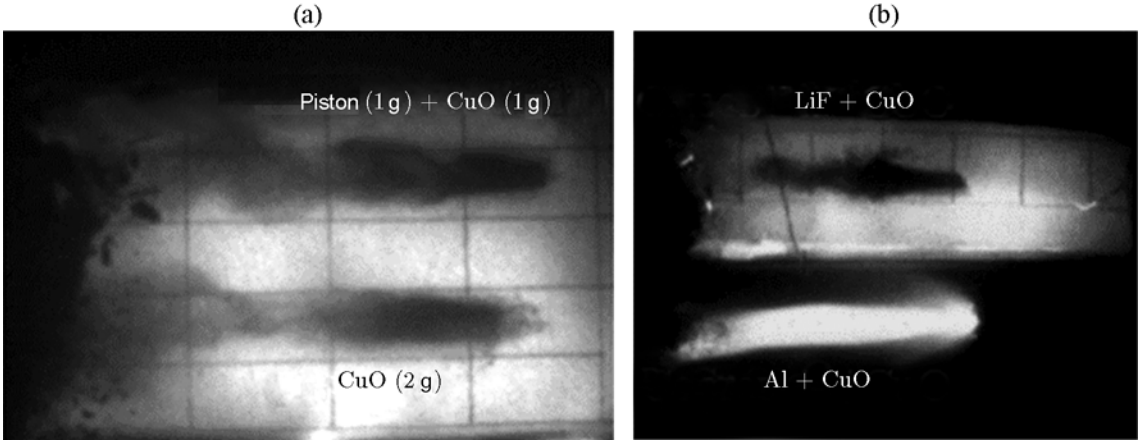

Fig. 6. Frames of high-speed photography of the product expansion process (time from left to right): (a) simultaneous explosive loading of inert CuO pellets (nozzle $S_n = S_0$; moment of photography 1700 μs); (b) simultaneous explosive loading of inert (LiF + CuO) and reactive (Al + CuO) mixtures (nozzle $S_n = 0.5S_0$; moment of photography 2150 μs).

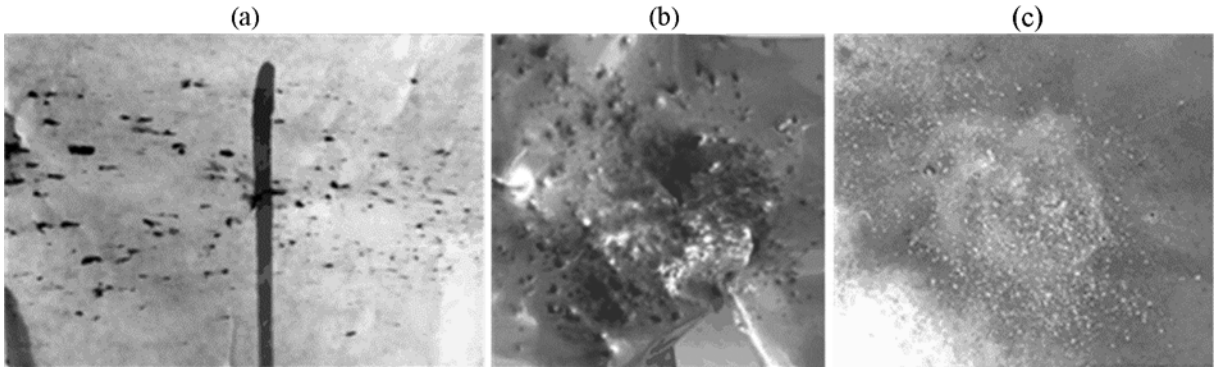

Fig. 7. Photographs of track impressions of the dispersed material of pellets on a paper screen and witness foils (a) and impressions of the inert pellet material (b) and reaction products of a burned pellet (c).

of x–t diagrams constructed on the basis of 8–12 photographs. Visualization of the flow indicates that it has a heterogeneous structure.

In the case of chemical interaction between components, the formation of particle flow occurs in the same way, as seen in frames of simultaneous high-speed photography of the shock loading of two other experimental assemblies (Fig. 6b). The top of the photograph shows the dark flow (velocity 491 m/s) of the pellet material consisting of an inert mixture of LiF + CuO (LiF is close in compressibility and density to Al and is used as its inert analog). The bottom of the photograph shows the glowing flow of reaction products of the Al + CuO thermite composition (velocity 499 m/s). Loading of pellets of inert and reactive components occurred under the same conditions. The similar dynamics of both flows implies that the release of chemical energy in the particle flow practically does not affect its velocity, which is determined only by the energy of the explosive charge and flow conditions. This conclusion is supported by the results of experiments on explosive loading of both the pure thermite mixture and the mixture diluted with an inert material (sand with a particle size of ≈200 μm) in proportions of 75/25 and 50/50. For a nozzle area $S_n = S_0$, the average velocity of the glowing front in these experiments was 460 ± 10 m/s at 600 μs.

Numerous track impressions on a paper surface located along the flow (Fig. 7a) and on witness foils located across the flow at a distance of ≈200 mm (Figs. 7b and 7c) confirm the presence of dispersed pellet material in the flow in the cases of both inert and reactive flows [22]. Single tracks (up to 10 pcs) are observed on the witness foil at a distance of 2000 mm.

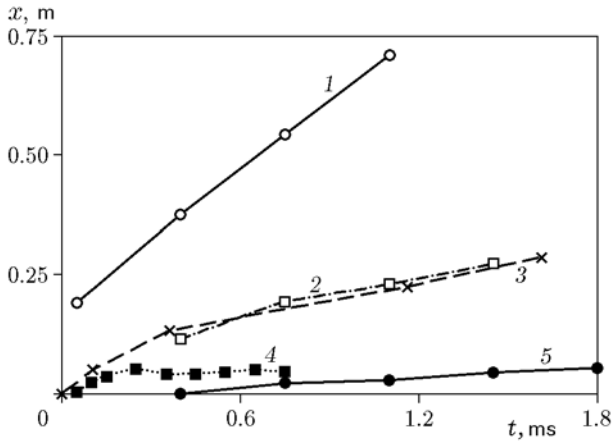

Fig. 8. Dynamics of various parts of the glow region: (*1*) flow front (average velocity 490 m/s); (*2*) center of the flow (145 m/s); (*3*) conductive flow front (164 m/s); (*4*) flow radius; (*5*) rear part of the flow (37 m/s).

FLOW DYNAMICS AND PARAMETERS

A characteristic feature of the chemical reaction in the flow is the bright glow of the products. The propagation dynamics of the glow region was determined from the results of high-speed photography with an CORDIN-222-16 electron-optical camera. In addition, we used chronograms of the closure of potential electrodes placed along the product expansion path by ionized products. Figure 8 shows the characteristic dynamics of various sections of the glow region.

The expansion velocity and the volume of ejected pellet material increase with increasing area of the nozzle orifice in the steel plate (Fig. 9). Thus, the initial velocity of the glow region of the flow increases from about 150 to 650 m/s with increasing diameter of the nozzle orifice, and the rate of increase in the longitudinal section area of the glow region reaches 35 $\text{mm}^2/\mu\text{s}$ at a time of 200 μs. Based on to the data set in Fig. 9, a relative nozzle area of $0.5S_0$ was selected as the most effective for use in subsequent experiments.

The inclusion of the air gap between the explosive charge and the assembly elements changes the loading pattern from shock-wave loading to pulsed loading with deceleration of detonation product flow. However, in the range of gap lengths used, the presence of gaps did not affect the ejection velocity of the pellet material for times of up to 300 μs. For all variants of the air gap length and for a nozzle area $S_n = S_0$, the flow velocity was 450 ± 20 m/s.

Originally, it was assumed that the initial parameters of the thermite pellet (particle size, time of preliminary mechanical activation, porosity) can affect the initiation and progress of chemical interaction between the components and, accordingly, the dynamics of the glow region. Experimental data on the propagation velocity of the glow region under shock loading of thermite pellets with different initial characteristics are shown in the table. The experimental results show that up to about 600 μs, the time of preliminary mechanical activation of the mixture, the porosity of the pellet, and the dilution with inert material does not affect the dynamics of the glow region.

Then, the longitudinal section area of the glow region decreases with the decrease being most rapid for pellets with the mixture activated for 6 and 8 min, which, according to [15], have the highest burning rates. Apparently, the mutual displacement of particles under shock-wave loading leads to activation of chemical reaction on the contact surface between the metal and oxidizer particles that exceeds the effect of preliminary mechanical activation.

For pellets of the mixture of nanosized components, a decrease in the initial flow velocity and faster completion of the chemical reaction are observed. This may be due to the greater energy dissipation of the initiating shock wave in the pellet with a larger specific particle surface.

Similar flow dynamics of the dispersed pellet material and the glow regions outside the nozzle of one section is obviously due to the constancy of the explosive charge energy. Thus, the stability of the energy and structural conditions for shock loading of thermite pellets with different technological preparation eliminates this difference during initiation and progress of the thermite reaction in the flow.

The dynamics of the brightness temperature of the flow was controlled along the propagation line using a four-channel pyrometer at wavelengths of 500, 600, 700, and 800 nm (Fig. 10). The maximum brightness temperature of the flow at the beginning of the trajectory averaged over wavelengths is 3500 K. The further decrease in the brightness temperature of the flow is 1.65 $\text{K}/\mu\text{s}$. Thermal effect (in the form of blue–violet discoloration) on a stainless steel foil 0.1 mm thick on the wall of the 90 mm diameter channel is observed at a distance of up to 450 mm. For stainless steel, this discoloration corresponds to a temperature of 600°C.

The high brightness temperature of the products suggests the presence of ionized particles in the flow. The specific electrical impedance evaluated from the conduction current pulses between the potential electrodes with a specified potential difference has an order of magnitude of $\approx 10^7\ \Omega \cdot \text{mm}^2/\text{m}$, which indicates a low degree of ionization of products. Cooling the flow results in condensation of reaction products (Fig. 11) in

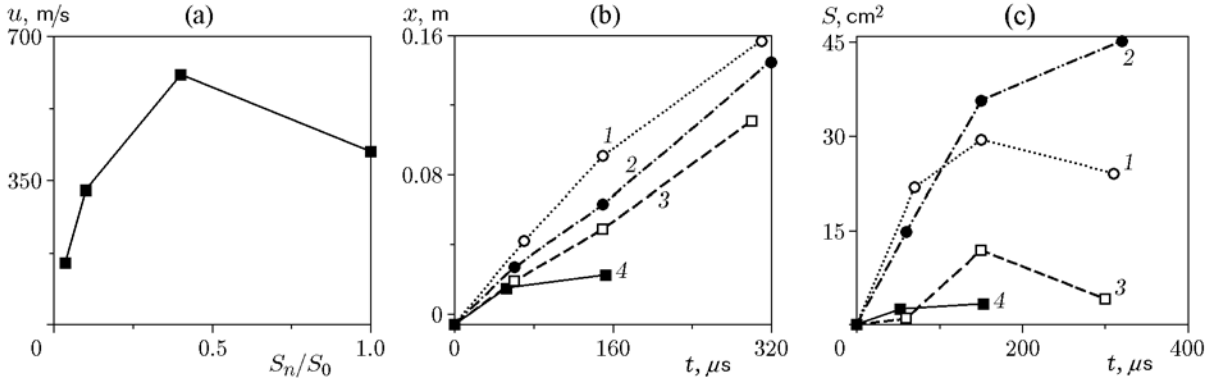

Fig. 9. Effect of the nozzle orifice area on the flow velocity (a) and the dynamics of the volume of the ejected pellet material (b and c) for $S_n = S_0$ (*1*), $0.4S_0$ (*2*), $0.1S_0$ (*3*), and $0.01S_0$ (*4*): x is the coordinate of the head of the product cloud and S is the maximum section of the product cloud.

Results of experiments

No.	Parameter	Parameter range		Result		
1	Time of mechanical activation of the mixture for $S_n = S_0$	2–20 min		Average flow velocity at 300 μs 475 ± 15 m/s Deflection of a steel plate 2.5 mm thick 5.5 ± 0.2 mm		
2	Porosity of the pellet for $S_n = 0.5S_0$	10–36%		Initial flow velocity 650 ± 20 m/s		
3	Initial particle size of the mixture for $S_n = S_0$			Flow velocity, m/s, at times		
				250 μs	500 μs	700 μs
		Nanosize		590	563	386
		Micron size		645	527	480
4	Bulk density mixture (mass 1 g)	Porosity 60%	$S_n = 0.5S_0$	Initial flow velocity 675 m/s		
			$S_n = S_0$	Average velocity at 600 μs 474 m/s		
5	Mixture of thermite composition and bulk density sand (mass 1 g) for $S_n = S_0$	25% sand		Average velocity at 600 μs 466 m/s		
		50%		Average velocity at 600 μs 460 m/s		
		75%		Average velocity of the middle part of the flow 270 m/s		

the form of various particles. In this case, Cu condenses both in the form of free nanosized particles and in the form of micron-sized droplets solidified on the surface of Al_2O_3 particles. Al_2O_3 oxide condenses mainly in the form of micron-sized spherical particles (≈10 μm), whose surface consists of smaller sticky particles.

Thus, the experimental results indicate that the short-term (1–2 μs) shock-wave loading of the 1 g porous pellet of a thermite mixture of Al and CuO powders was accompanied by energy dissipation in it ≈20 J, leading to the initiation of chemical interaction between the components of the mixture with subsequent long

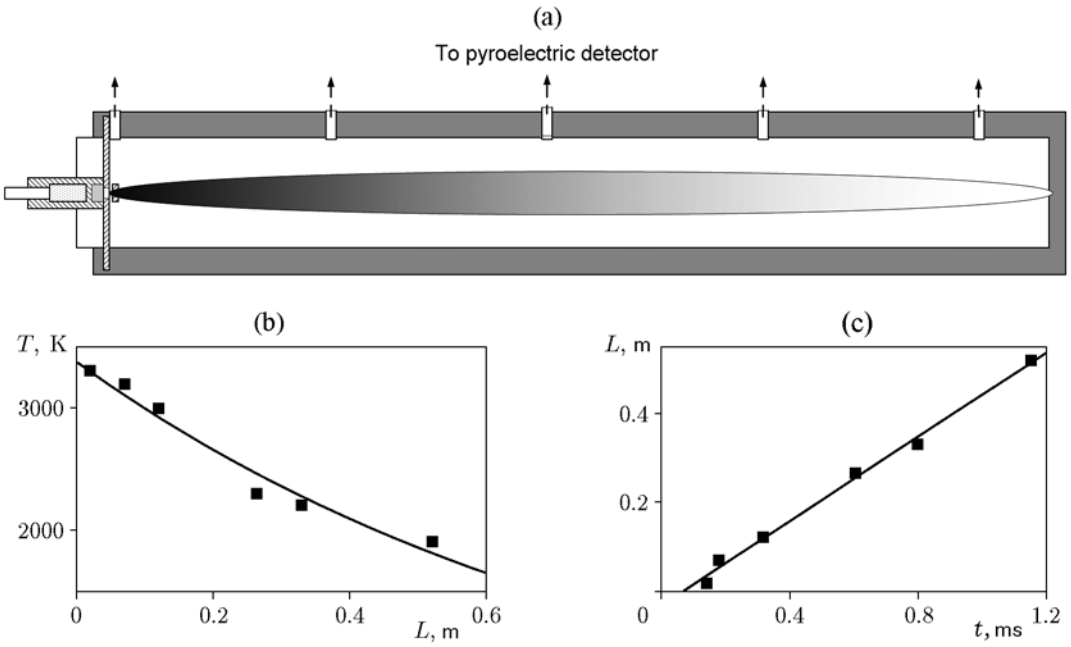

Fig. 10. Schematic diagram of the experiment to measure the brightness temperature of the reaction products of the mixture (a), the brightness temperature distribution along the flow direction of the pellet material (b), and a chronogram of the propagation of the front of the glow region (474 m/s) based on measurements of the brightness temperature of combustion products (c).

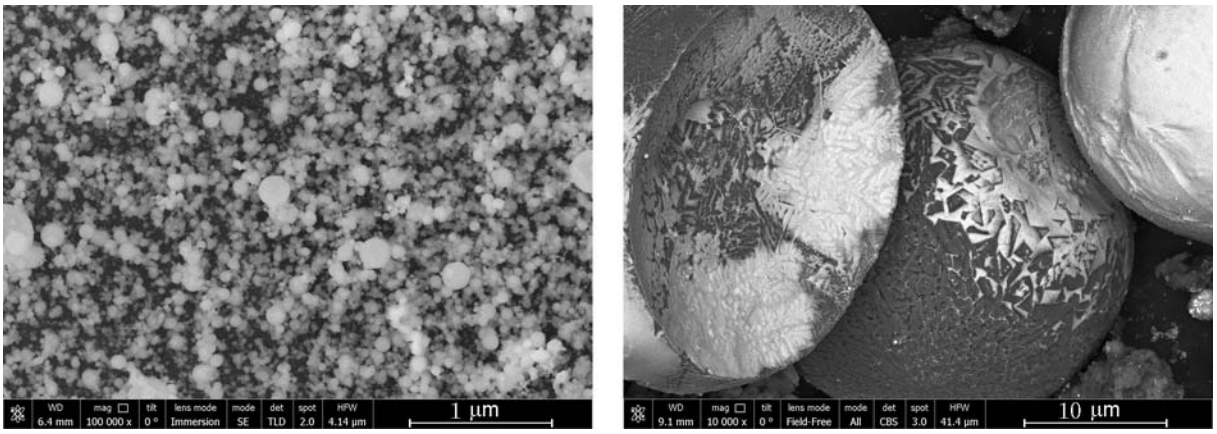

Fig. 11. Photographs of reaction products: light inclusions are Cu nanoparticles, and gray inclusions are spherical Al_2O_3 particles with copper solidified on the surface.

(4–5 ms) afterburning. Initiation of the reaction does not affect the loading parameters during the passage of the shock wave in the pellet. This casts doubt on the conclusion that the initiated exothermic chemical interaction was responsible for the kinks in D–u and p–u diagrams found in [16] for pressed pellets of a mixture of Al and CuO powders.

INITIATION OF A THERMITE REACTION IN A DETONATION WAVE

It was previously noted that preliminary mechanical activation in ball mills and subsequent pressing of the mixture provide equalization of the original particle sizes (difference within one order of magnitude). It can be suggested that shock loading through a steel pis-

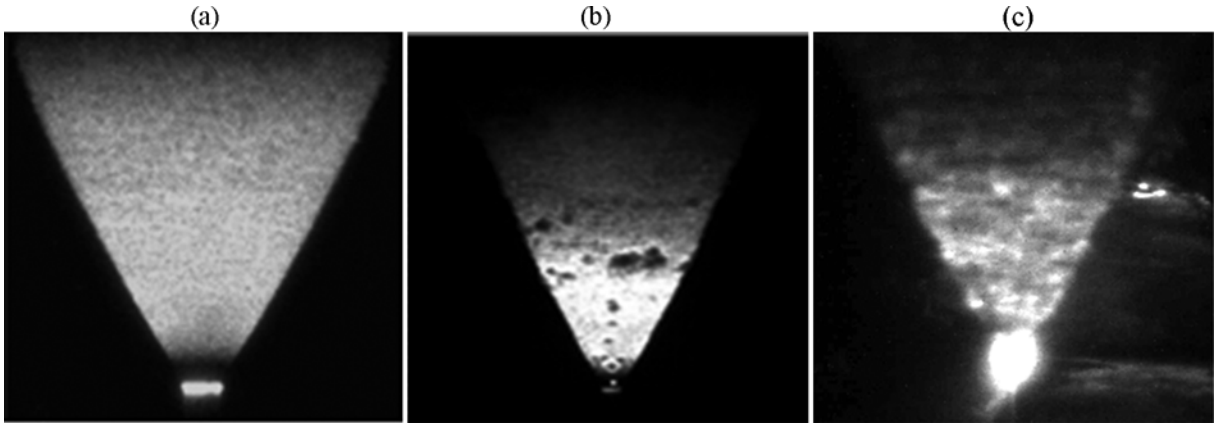

Fig. 12. Photographs of the detonation of cylindrical charges: (a) RDX powder (1.15 g/cm^3); (b) water-filled RDX powder (20/80; 1.2 g/cm^3); (c) mixture of a pyrotechnic Al + CuO composition with RDX powder in a mass ratio of 40/60.

ton leads to predominantly one-dimensional (accurate to the particle size of the components) impact on the pressed thermite pellet. To implement bulk loading of particles of the thermite composition, it is necessary to eliminate the effect of dynamic compression by the steel piston and dilute the mixture with particles of much larger sizes. This can be done, e.g., by placing composite particles of the activated thermite composition among large particles of the explosive powder. Such experiments were conducted for a mixture of the thermite composition with phlegmatized RDX powder (particle size 100–150 μm). In the experiments, we used mixtures of the explosive and thermite composition in a mass ratio of 20/80, 30/70, 40/60, and 50/50. These mixtures were poured into a glass tube with a diameter of 8.5 mm and compacted to a relative density of $\approx$0.75. The charge height was 100 mm. Detonation was initiated by charges of phlegmatized RDX with a height of 100 mm and a density of $\approx$1.2 g/cm^3 placed in the same tube. The RDX charge detonated at a velocity of 6.53 km/s. In the experiments, the glow of the front and the expansion of detonation products were recorded. The results showed that in the first three compositions, normal detonation at velocities of 5.7, 5.2, and 4.3 km/s, respectively, occurred. Initiation of a mixture of the Al + CuO composition with RDX in a ratio of 50/50 leads to the formation of a detonation-like process with a low velocity of about 1.5 km/s. The characteristic moment of expansion of detonation products of the 40/60 composition is presented in Fig. 12 in comparison with photographs of the detonation of cylindrical charges of powdered and water-filled RDX.

The photographs show the glow of the expansion cones of detonation products. The expansion of detonation products of powdered RDX (Fig. 12a) is characterized by a uniformly granular glow structure which reflects the uniform distribution of pores and explosive particles in the charge. The bright expansion cone of detonation products of water-filled RDX (Fig. 12b) contains dark inclusions apparently due to the vapor of the boiling water component of the original explosive charge. The photograph of the expansion of detonation products of the mixture of RDX with the thermite composition (Fig. 12c) is filled with bright dots obviously associated with a local chemical energy release in expanding clusters of the thermite mixture. The vertex angles of the product expansion cones in Figs. 12a, 12b, and 12c are 59, 50, and 48° respectively, which is due to the different density of the additional components of the charge.

Thus, it was found that the shock-wave loading of the Al + CuO thermite compositions initiated combustion in the case of plane shock-wave loading as well as in explosion products.

CONCLUSIONS

1. A quantitative characteristic of the shock-wave initiation and combustion dynamics of mixtures of aluminum with copper oxide: at a shock loading time of 1–2 μs, the chemical reaction of the components lasts at least 4–5 ms.

2. Chemical interaction of the components under shock-wave loading occurs mainly in expanding products with the formation of a glow region with a brightness temperature of $\approx$3500 K.

3. Based on the set of data of high-speed photography, triggering waveforms of electrical contact pins, and track impressions on thin witness foils, the glow region

should be characterized as the expanding flow of reacting clusters and cold components of the mixture in the cloud of radiating plasma of combustion products.

4. The factor initiating a chemical reaction in the flow of the mixture of reactive powdered components after shock loading of the pressed pellet are expanding clusters carrying primary sites of the chemical reaction.

5. The duration of the glow (chemical reaction) region is due to:
—the multi-site initiation of the reaction under shock loading;
—the reaction propagation rate in the contact zone of the components;
—the cluster nature of the dispersion of the compressed pellet;
—the small size of the site compared to the contact area of the components in the cluster.

Initiation of the thermite composition in a mixture with the detonating powder explosive (RDX) is also accompanied by multi-site combustion of expanding detonation products in the environment.

This work was performed using the equipment of the unique Sfera facility at the Joint Institute for High Temperatures RAS.

REFERENCES

1. A. F. Belyaev, *Combustion, Detonation, and Work of Explosion of Condensed Systems* (Nauka, Moscow, 1968) [in Russian].
2. S. P. Smirnov, E. V. Kolganov, V. P. Il'in, Ya. S. Kulakevich, A. S. Smirnov, and F. T. Khvorov, "Development of Explosive Compositions of Increased Efficiency with Satisfactory Performance," in *V Khariton Scientific Readings: Proc. Int. Conf.* (RFNC-VNIIEF, Sarov, 2003), pp. 231, 232.
3. A. A. Kotomin, "Elastic Explosive Materials," Ross. Khim. Zh. **41** (4), 89–101 (1997).
4. V. K. Bobolev, I. A. Karpukhin, and V. A. Teselkin, "Mechanism of Initiation of an Explosion by Impact in Mixtures of Ammonium Perchlorate with Combustible Additives," Fiz. Goreniya Vzryva **7** (2), 261–264 (1971) [Combust., Expl., Sock Waves **7** (2), 221–223 (1971)].
5. M. F. Gogulya and M. A. Brazhnikov, "On the Characteristic Times of Chemical Reactions in Heterogeneous Systems under Dynamic Loading," Khim. Fiz. **13** (11), 88–101 (1994).
6. S. I. Gerasimov, Yu. I. Faikov, and S. A. Kholin, *Cumulative Light Sources* (RFNC-VNIIEF, Sarov, 2011).
7. A. A. Kotomin, V. V. Efanov, S. A. Dushenok, A. S. Kozlov, M. A. Trapeznikov, E. N. Breshev, and V. V. Gorovtsov, "Controlling the Detonability of Explosive Materials Used in Spacecraft Separation Systems," Vestn. NPO Lavochkina **13** (2), 12–18 (2012).
8. A. I. Aniskin, "Detonation of Explosive Mixtures with Aluminum," *Detonation and Shock Waves* (Inst. of Chem. Phys., USSR Acad. of Sci., Chernogolovka, 1986), pp. 26–31.
9. I. M. Voskoboinikov, "Oxidation of Aluminum in Shock and Detonation Waves," Khim. Fiz. **28** (12), 40–44 (2009).
10. A. A. Borisov, A. A. Sulimov, M. K. Sukoyan, P. V. Komissarov, I. O. Shamshin, R. Kh. Ibragimov, and Yu. M. Mikhailov, "Blast Waves in Open Space upon Non-Ideal Detonation of High-Density Mixed Compositions Enriched in Aluminum," Khim. Fiz. **28** (11), 59–68 (2009).
11. Fan Yang, Xiaoli Kang, Jiangshan Luo, Zao Yi, and Yongjian Tang, "Preparation of Core-Shell Structure $KClO_4$@Al/CuO. Nanoenergetic Material and Enhancement of Thermal Behavior," Sci. Report No. 7 (2017), Article number 3730; DOI: 10.1038/s41598-017-03683-z.
12. A. Yu. Dolgoborodov, A. N. Streletskii, M. N. Makhov, I. V. Kolbanev, and V. E. Fortov, "Explosive Compositions Based on Mechanically Activated Metal–Oxidizer Mixtures," Khim. Fiz. **25** (12), 40–45 (2007).
13. A. N. Dremin, S. D. Savrov, V. S. Trofimov, and K. K. Shvedov, *Detonation Waves in Condensed Media* (Nauka, Moscow, 1970) [in Russian].
14. B. G. Loboiko and S. N. Lyubyatinskii, "Reaction Zones of Detonating Solid Explosives," Fiz. Goreniya Vzryva **36** (6), 45–64 (2000) [Combust., Expl., Sock Waves **36** (6), 716–732 (2000)].
15. A. Yu. Dolgoborodov, V. G. Kirilenko, A. N. Streletskii, I. V. Kolbanev, A. A. Shevchenko, B. D. Yankovskii, S. Yu. Anan'ev, and G. E. Val'yano, "Mechanically Activated Al/CuO Thermite Composition," Gorenie Vzryv **11** (3), 103–113 (2018).
16. V. A. Golubev, V. V. Vakhrushev, E. V. Panturov, B. E. Grinevich, A. V. Strikanov, A. A. Uskov, V. A. Laktyushkin, V. A. Kozlov, O. S. Demidov, A. L. Ulanova, and V. V. Yaroshenko, "The Behavior of AlCuO Pyrotechnic Composition under Shock-Wave Loading," in *III Khariton Scientific Readings, Proc. Int. Conf.* (RFNC-VNIIEF, Sarov, 2002), pp. 75–80.
17. V. S. Solov'ev, "Some Specific Features of Shock-Wave Initiation of Explosives," Fiz. Goreniya Vzryva **36** (6), 65–76 (2000) [Combust., Expl., Sock Waves **36** (6), 734–744 (2000)].
18. M. A. Dmitrieva, "Model of a Shock-Loaded Reactive Powdered Body with Structure," Abstracts of Doct. Dissertation (Tomsk State University, Tomsk, 2009).

19. S. Y. Ananev, A. Y. Dolgoborodov, A. A. Shiray, B. D. Yankovsky, "Shock Initiation of Exothermic Reactions in Mechanically Activated Mixtures," J. Phys.: Conf. Ser. **774** (1), 1–8 (2016); DOI:10.1088/1742-6596/774/1/012069.
20. P. V. Pikhtovnikov and V. I. Zav'yalov, *Forming of Sheet Metal by Explosion* (Mashinostroenie, Moscow, 1964) [in Russian].
21. S. Y. Ananev, B. D. Yankovsky, and A. Y. Dolgoborodov, "The Combustion of Al–CuO Powder Mixture under Shock Wave Initiation of the Reaction," J. Phys.: Conf. Ser. **946** (1), 1–7 (2018).
22. S. Yu. Anan'ev, A. Yu. Dolgoborodov, and B. D. Yankovskii, "Dynamics of Expansion of Combustion Products of a Mechanically Activated Mixture of Aluminum with Copper Oxide," Gorenie Vzryv **10** (4), 81–85 (2017).